

# New methods for multiple testing in permutation inference for the general linear model

Tomáš Mrkvička<sup>1,2</sup>

*Faculty of Economics, University of South Bohemia, Czech Republic*

Mari Myllymäki

*Natural Resources Institute Finland (Luke), Helsinki, Finland*

Naveen Naidu Narisetty

*University of Illinois, Urbana-Champaign, USA*

---

## Abstract

Permutation methods are commonly used to test significance of regressors of interest in general linear models (GLMs) for functional (image) data sets, in particular for neuroimaging applications as they rely on mild assumptions. Permutation inference for GLMs typically consists of three parts: choosing a relevant test statistic, computing pointwise permutation tests and applying a multiple testing correction. We propose new multiple testing methods as an alternative to the commonly used maximum value of test statistics across the image which improve in terms of power and robustness and allow to identify the regions of potential rejection via a graphical output. The proposed methods rely on sorting the permuted functional test statistics based on pointwise rank measures. We developed the R package GET which can be used for computation of the proposed procedures.

*Keywords:* General linear model, Global envelope test, Graphical method, Multiple testing correction, Permutation inference

---

## 1. Introduction

General linear models (GLMs) are among the most commonly used statistical tools in the field of neuroimaging for analyzing imaging data (Christensen, 2002). To perform statistical inference based on GLMs, one approach is to use parametric methods which rely on stringent assumptions, particularly the normality of the random errors in the GLM and a number of assumptions under

---

<sup>1</sup>Corresponding author: mrkvicka.toma@gmail.com

<sup>2</sup>Dpt. of Applied Mathematics and Informatics, Faculty of Economics, University of South Bohemia, Studentská 13, 37005 České Budějovice, Czech Republic

which asymptotic distributions of the test statistics arise. Alternatively, one can use non-parametric methods with weaker assumptions about the data. Permutation tests are a class of non-parametric methods, which have a long history going back to Fisher (1935). Fisher demonstrated that the null hypothesis could be tested by observing, how often the test statistic computed from permuted observations would be more extreme than the same statistic computed without permutation. Even though the data in neuroimaging applications are commonly images, the same principle still holds. A detailed introduction to the permutation inference for the GLMs for neuroimage data can be found in Winkler et al. (2014).

Analysis based on permutation tests consists of several crucial steps. First, a suitable test statistic that is computed for each single spatial point of an image has to be chosen such that it is informative about the studied null and alternative hypotheses and which is homogeneous across the image. Second, the appropriate permutation scheme has to be used to generate the permutations from the studied null hypothesis. Finally, an appropriate multiple testing correction has to be applied on significance results obtained for all spatial points by the permutation test.

Commonly used test statistics include the  $t$  and  $F$  statistics, or the  $G$  statistic defined in Winkler et al. (2014) which generalises the classical statistics into various cases with heteroscedasticity. However, a serious limitation of the  $F$  or  $G$  statistics is that they are not pivotal across different locations of the image in terms of the entire distribution, but only in terms of the first and second moments when the errors are not normally distributed. Therefore, if the error distribution is non-normal and non-stationary across the image which occurs commonly in practice, the distribution of these test statistics varies across the image causing the desired quantiles of the test statistics to vary as well. If this heterogeneity is ignored, e.g. by taking the maximum  $F$  statistic across the spatial points as the test statistic, this can bring a substantial loss of power as we will demonstrate in our simulation study.

Due to the non-pivotal nature of the  $F$  and  $G$  statistics, a more suitable choice is the permutation  $p$ -value, which is automatically a pivotal statistic, i.e. its distribution does not change across the image. Therefore, it would be convenient to perform the multiple testing correction by taking the minimum  $p$ -value across the image as the test statistic. However, the permutation  $p$ -value has a serious disadvantage: due to its discreteness, the (minimum)  $p$ -values obtained from permutations contain ties and the resulting test tends to be conservative, leading to loss of power as well (Pantazis et al., 2005). This disadvantage is enormous especially in the case of high resolution images, as the number of permutations can not be large due to computational limitations.

Another problem arises for test statistics which accumulate the data from the surrounding area of a single spatial point, e.g. the local area above a given threshold around a spatial point. Namely, if the spatial autocorrelation of the data is inhomogeneous across the domain, then the sizes of the areas above the thresholds in different parts of the domain are not comparable. This problem was recently treated for special case of cluster size permutation tests in Hayasaka

et al. (2004) and Salimi-Khorshidi et al. (2011). In this paper we discuss solutions for the case of inhomogeneous spatial autocorrelation and also for the case of inhomogeneous distribution of the test statistic.

The classical multiple testing procedures, computing the maximum  $F$  or the minimum  $p$ -value statistic across all spatial points, control the family wise error rate (FWER) (e.g. Winkler et al., 2014). This paper introduces three new multiple testing corrections for the permutation inference for the GLMs, controlling the FWER in a similar manner. Another possibility is to control false discovery rate (FDR) (Benjamini and Hochberg, 1995) instead and use a FDR multiple comparison method on the computed  $p$ -values for each spatial point. We compare these approaches in our simulation experiment.

The new methods are alternative solutions to the ties problem of  $p$ -values. The first correction is based on the extreme rank length measure what was originally proposed by Myllymäki et al. (2017) and Narisetty and Nair (2016) for spatial and functional data analysis. The other two corrections rely on the continuous rank measure introduced in the technical report of Hahn (2015) and the area rank measure presented in this work first time. We carefully describe the homogeneity assumptions of the  $F$ -max,  $p$ -min and new methods and further their sensitivity to different types of extremeness of the test statistic. By a simulation study, we illustrate the power of the new and existing tests under different scenarios, both when the homogeneity assumptions of the multiple correction methods are met and when not. We show that the  $F$ -max and our proposed methods tend to be more powerful than the  $p$ -min and FDR approaches. In particular, we illustrate that the  $F$ -max method has high power under normality and homogeneity of the distribution of the test statistic, but when these assumptions were not met, then the proposed new methods have higher power. A further asset of the new methods, namely a graphical interpretation of the test results in a similar manner as in global envelope testing (Myllymäki et al., 2017; Mrkvička et al., 2016; Mrkvička et al., 2018), is illustrated by a simulated example of 2D images, where the  $F$  statistic is not pivotal. We conclude that the choice of the measure for multiple correction should be done on the basis of reasonable assumptions of different types of homogeneity, and the expected type of extremeness of the test statistic.

## 2. Multiple testing correction for permutation methods

Let us consider the general linear model

$$\mathbf{Y}(r) = \mathbf{X}(r)\beta(r) + \mathbf{Z}(r)\gamma(r) + \epsilon(r),$$

where the argument  $r \in I \subset \mathbb{R}^d$  determines a spatial point or voxel of the image or generally an argument of  $d$ -dimensional functions. The number of arguments  $r \in I$  will be denoted by  $N$ . For every argument  $r$ , we consider a one-dimensional GLM with  $\mathbf{X}(r)$  being a  $n \times k$  matrix of regressors of interest,  $\mathbf{Z}(r)$  being a  $n \times l$  matrix of nuisance regressors,  $\mathbf{Y}(r)$  being a  $n \times 1$  vector of observed data and  $\epsilon(r)$  being a  $n \times 1$  vector of random errors with mean zero

and finite variance  $\sigma^2(r)$  for every  $r \in I$ . Further assumptions about the error structure will be given along the definitions of the multiple correction methods below. Further,  $\beta(r)$  and  $\gamma(r)$  are the regression coefficient vectors of dimensions  $k \times 1$  and  $l \times 1$ , respectively. Often factors are given for the whole image, in which case the regressors do not depend on the index  $r$  and so the matrices  $\mathbf{X}(r)$  and  $\mathbf{Z}(r)$  are identical for every  $r \in I$ . However, this simplification is not necessary. The null hypothesis to be tested is

$$H_0 : \mathbf{C}(r)\beta(r) = 0, \quad \forall r \in I,$$

where  $\mathbf{C}(r)$  is a  $t \times k$  matrix of  $t$  contrasts of interest.

The GLM setup includes a wide range of applications in neuroimaging, see Winkler et al. (2014) for worked examples. Under various setups, a nonparametric pointwise permutation test can be applied to obtain a set of  $p$ -values,  $\{p_r : r \in I\}$ . We refer to the detailed description of pointwise permutation tests in Winkler et al. (2014). Shortly, first a test statistic  $T(r)$  is chosen from a vast number of possibilities, reflecting the tested null model  $H_0$  and heteroscedasticity. A common choice is the  $F$  statistic (Christensen, 2002). Then permutations are used to obtain the distribution of  $T(r)$  under the null hypothesis  $H_0$ . The choice of the permutation scheme is important for the performance of the method. We chose the permutation of the residuals under the null model (Freedman and Lane, 1983), which is approximate, but according to Anderson and Ter Braak (2003) (see also Winkler et al., 2014) it is the most precise permutation method in the case of nuisance effects. The last step is to apply a multiple testing correction.

Following sections describe various multiple testing corrections in these permutation procedures. We assume that the same  $J$  permutations have been applied for every argument  $r \in I$ .

### 2.1. $p$ -min approach

First, the minimum  $p$ -value is calculated for the original data,

$$p_0^{\min} = \min_{r \in I} p_r.$$

Then the same statistic,  $p_j^{\min}$ , is computed for every permutation  $j, j = 1, \dots, J$ , as the permuted data were original data. Second, the Monte Carlo  $p$ -value

$$p^{\min} = \frac{1}{J+1} \sum_{j=0}^J \mathbb{I}(p_j^{\min} \leq p_0^{\min})$$

is calculated. Here  $\mathbb{I}$  denotes the indicator function.

The pointwise  $p_r$ -values are pivotal, therefore the  $p$ -min approach needs no further assumptions about the random error  $\epsilon(r)$ . However, since the  $p$ -values of the permutation test can achieve only values  $\frac{1}{J+1}, \frac{2}{J+1}, \dots, 1$ , many ties can appear among  $p_0^{\min}, p_1^{\min}, \dots, p_J^{\min}$ , especially for large  $N$ , leading to a conservative test. A possible solution to solve this problem is to randomize the effect of ties, but for large  $N$  this test is then mainly driven by this random effect.

## 2.2. Refinements of the $p$ -min approach

The  $p$ -min approach is in fact equivalent to the global rank envelope test defined by Myllymäki et al. (2017) for spatial processes: In the global test, the test statistic  $T(r), r \in I$ , is computed for the data  $(T_0(r))$  and for the permutations  $(T_j(r), j = 1, \dots, J)$ . Every  $T_j(r), j = 0, \dots, J$ , is equipped with the extreme rank measure which after a certain normalization is equivalent to the  $p_j^{\min}$ .

In the sequel we propose the following three methods for breaking the ties between the  $p_j^{\min}$  values:

- The extreme rank length approach takes into account the number of minimal  $p$ -values,
- the continuous rank approach measures the size of extremeness of  $T(r)$  that is associated with the  $p^{\min}$ , and
- the area rank takes into account both of the above aspects.

The measures and the corresponding global envelopes are defined here as one-sided since the extremeness of the test statistic  $T(r)$  used in the GLM is usually realized only for high values.

### 2.2.1. Extreme rank length

The extreme rank length (Myllymäki et al., 2017; Narisetty and Nair, 2016; Mrkvička et al., 2018) refines the  $p$ -min approach in the sense that not only the  $p_j^{\min}$  itself but also the number of  $p_r$  which are equal to  $p_j^{\min}$  are taken into account. To define the extreme rank length measure formally, consider the vectors of pointwise ordered  $p$ -values  $\mathbf{p}_j = (p_{[1]j}, p_{[2]j}, \dots, p_{[N]j})$ , where  $\{p_{[1]j}, \dots, p_{[N]j}\} = \{p_{1j}, \dots, p_{Nj}\}$  and  $p_{[k]j} \leq p_{[k']j}$  whenever  $k \leq k'$ . The extreme rank length measure is equal to

$$e_j = \frac{1}{J+1} \sum_{j'=0}^J \mathbb{I}(\mathbf{p}_{j'} \prec \mathbf{p}_j), \quad (1)$$

where

$$\mathbf{p}_j \prec \mathbf{p}_{j'} \iff \exists n \leq N : p_{[n]j} < p_{[n]j'} \text{ and } p_{[k]j} = p_{[k]j'} \forall k < n.$$

Since the probability of having a tie in the extreme rank length measure is rather small, the application of Monte Carlo test on the extreme rank length solves the ties problem (see also Myllymäki et al., 2017). Thus the final  $p$ -value is  $p^{\text{erl}} = \frac{1}{J+1} \sum_{j=0}^J \mathbb{I}(e_j \leq e_0)$ .

Since the extreme rank length summarizes the minimal  $p$ -values over  $r \in I$ , it has to assume that the correlation structure of the test statistic is homogeneous. This means that the correlation structure of the error term  $\epsilon(r)$  must be homogeneous or the test statistic has to account for the inhomogeneity in the error term.

Figure 1 illustrates the refinements of the  $p$ -min approach, namely how the ties are broken for the two one dimensional test statistics  $T(r)$  (the black and grey thick solid lines) that both obtain most extreme values in the considered set of functions for some  $r \in I$ . The extreme rank length measure counts  $r \in I$  (denoted by crosses) at which the test statistics obtain their most extreme rank. Thus, by the extreme rank length measure, the black function is regarded as a more extreme function than the grey one.

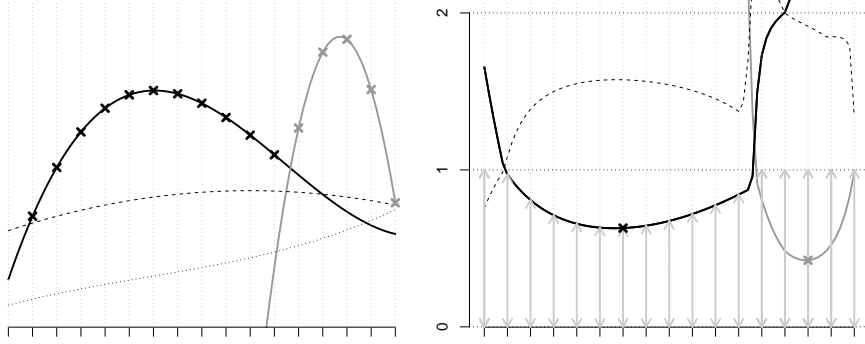


Figure 1: Illustration of how the ties are broken by the extreme rank length, continuous and area measures for two test statistics (black and grey thick lines) that both are most extreme (largest values) functions for some  $r$ . The statistics are evaluated at  $r$  shown by ticks at x-axes and dotted vertical lines. The details are explained in the text.

### 2.2.2. Continuous rank

Another refinement of  $p^{\min}$  we propose is the continuous rank measure  $c_j = \min_i c_{rj} / J$ , where  $c_{rj}$  is the continuous pointwise rank that is based on the relative magnitude of the test statistic  $T_j(r)$  with respect to the other  $T_{j'}(r)$ ,  $j' = 0, \dots, J$ , as follows:

$$c_{rj} = \sum_{j'} \mathbb{I}(T_{j'}(r) > T_j(r)) + \frac{T_{[j-1]}(r) - T_j(r)}{T_{[j-1]}(r) - T_{[j+1]}(r)} \quad \text{for } j : T_j(r) \neq \max_{j'} T_{j'}(r) \\ \text{and } T_j(r) \neq \min_{j'} T_{j'}(r), \\ c_{rj} = \exp \left( -\frac{T_j(r) - T_{[j+1]}(r)}{T_{[j+1]}(r) - \min_j T_j(r)} \right) \quad \text{for } j : T_j(r) = \max_{j'} T_{j'}(r), \\ c_{rj} = J \quad \text{for } j : T_j(r) = \min_{j'} T_{j'}(r).$$

Here  $T_{[j+1]}(r)$  denotes the value of a test statistic which is the one just below  $T_j(r)$  in magnitude at argument  $r$  and  $T_{[j-1]}(r)$  denotes the value of a test statistics which is the one just above  $T_j(r)$  at  $r$ , i.e.  $T_{[j+1]}(r) = \max_{j': T_{j'}(r) < T_j(r)} T_{j'}(r)$  and  $T_{[j-1]}(r) = \min_{j': T_{j'}(r) > T_j(r)} T_{j'}(r)$ . When the probability to have ties among  $T_j(r)$ ,  $j = 0, \dots, J$ , is zero, then the probability to have ties among  $c_j$

is zero as well. In the case of ties among  $T_j(r), j = 0, \dots, J$ , the continuous pointwise rank  $c_{rj}$  is computed just as a pointwise rank, by averaging these ties. Finally, the univariate Monte Carlo test is performed based on  $c_j$ . Thus the final  $p$ -value is  $p^{\text{cont}} = \frac{1}{J+1} \sum_{j=0}^J \mathbb{I}(c_j \leq c_0)$ .

The pointwise continuous ranks, and thus the continuous rank  $c_j$ , are based on the values of the test statistic  $T_j(r)$  relative to the other values at  $r, r \in I$ , and not only at ranks, therefore the assumption of homogeneity of  $T(r)$  is required as in the case of the  $F$ -max procedure. The difference in these two procedures is that the continuous rank depends on  $T(r)$  values only in the part of the procedure which breaks the ties of the  $p_j^{\text{min}}$ -values. So in order to satisfy the pivotality of  $c_{rj}$  across  $r \in I$  the error term  $\epsilon(r)$  has to be homogeneous or normal.

Figure 1 further shows the pointwise continuous ranks in the right plot for the same test statistics as in the left plot (black and grey thick lines). These ranks are defined on the basis of the vertical differences of the function and next function scaled appropriately as specified above. For each  $r$ , the most extreme function obtains a continuous rank  $< 1$ . The (overall) continuous rank is obtained as the minimum of the pointwise continuous ranks, thus being about  $0.6/J$  and  $0.4/J$  for the black and grey test statistics, respectively (denoted by black and grey crosses in Figure 1, right). Thus, according to the continuous rank measure, the grey test statistic is more extreme than the black test statistic.

### 2.2.3. Area rank

The last refinement which we consider is the area rank measure  $a_j$  obtained as:

$$a_j = \frac{1}{JN} \sum_r \min((J+1) \min_r p_{rj}, c_{rj}), \quad (2)$$

where  $N$  is equal to the number of  $r \in I$ .

The univariate Monte Carlo test is performed based on  $a_j$  with  $p^{\text{area}} = \frac{1}{J+1} \sum_{j=0}^J \mathbb{I}(a_j \leq a_0)$ .

Because the area measure combines the extreme rank length and continuous measures into one, it inherits their assumptions, i.e. homogeneity of the correlation structure and homogeneity of the distribution of the test statistic. Nonetheless, from our simulation study it appears that the area measure is the most robust to violating these two assumptions, due to its combined nature.

Figure 1 (right) also illustrates the area rank measure: the light grey vertical arrows correspond to the summands (multiplied by  $JN$ ) in the formula (2) for the thick black test statistic. For the grey statistic the area measure is calculated similarly. In this considered case, the black statistics is slightly more extreme.

### 2.2.4. Graphical interpretation - $100 \cdot (1 - \alpha)\%$ global envelope

Myllymäki et al. (2017) defined the graphical global envelope with respect to the extreme rank ordering. Because the extreme rank ordering may have a lot of ties, we present global envelopes based on the proposed measures of extreme rank length, continuous rank and area rank orderings which aim to avoid the

ties. These global envelopes retain the graphical interpretation of the envelope, which is shown in the next theorem.

Consider any of the three measures we defined and denote them using a common notation  $M_j, j = 0, \dots, J$ . Let  $I_\alpha = \{j \in 0, \dots, J : M_j \geq M_{(\alpha)}\}$  be the index set of vectors, where the threshold  $M_{(\alpha)}$  is chosen to be the largest value in  $\{M_0, \dots, M_J\}$  for which

$$\sum_{j=0}^J \mathbb{I}(M_j < M_{(\alpha)}) \leq \alpha(J+1), \quad (3)$$

and define the global envelope as

$$T_{\text{low}}^{(\alpha)}(r) = -\infty, \quad T_{\text{upp}}^{(\alpha)}(r) = \max_{j \in I_\alpha} T_j(r).$$

We get the global envelope such that, the probability that  $T_0(r)$  falls outside this envelope in any of the  $r$  points is less or equal to  $\alpha$ ,

$$\Pr(\exists r \in I : T_0(r) \notin [T_{\text{low}}^{(\alpha)}(r), T_{\text{upp}}^{(\alpha)}(r)]) \leq \alpha.$$

The following theorem states that inference based on the  $p$ -value  $p^M$  (where  $p^M$  stands for  $p^{\text{erl}}, p^{\text{cont}}$  and  $p^{\text{area}}$ ) and on the global envelope specified by  $T_{\text{low}}^{(\alpha)}(r), T_{\text{upp}}^{(\alpha)}(r)$  with respect to the appropriate measure are equivalent. Therefore, we can refer to these envelopes as the  $100 \cdot (1 - \alpha)\%$  global *extreme rank length envelope*, *continuous rank envelope* and *area rank envelope*.

**Theorem 2.1.** *Assume that there are no pointwise ties with probability 1 among  $T_j(r), j = 0, \dots, J$ . Then*

1.  $T_0(r) > T_{\text{upp}}^{(\alpha)}(r)$  for some  $r \in I$  iff  $p^M \leq \alpha$ , in which case the null hypothesis is rejected;
2.  $T_0(r) \leq T_{\text{upp}}^{(\alpha)}(r)$  for all  $r \in I$  iff  $p^M > \alpha$ , and thus the null hypothesis is not rejected;

*Proof.* According to the definition of  $p^M$ ,  $p^M \leq \alpha$  iff number of  $M_j$  smaller or equal to  $M_0$  is smaller or equal to  $\alpha(J+1)$ . That is equivalent, according to the definition of  $M_{(\alpha)}$  to  $M_0 < M_{(\alpha)}$ . This holds iff  $0 \notin I_\alpha$ , which is equivalent to  $T_0(r) > T_{\text{upp}}^{(\alpha)}(r)$  for some  $r \in I$  according to the definition of the measure  $M$ .

The second part of the proof can be proven similarly. □

### 2.3. $F$ -max approach

Usually the statistic  $T(r)$  is one of the statistisc used in the parametrical general linear models, i.e.  $t$  statistic,  $F$  statistic, or variance weighted  $F$  statistic. In these cases, an immediate solution to the problem of ties is to replace  $p^{\text{min}}$  statistic in the Monte Carlo test directly by the  $F^{\text{max}} = \max_{r \in I} T(r)$  statistic. The assumption of homogeneity of  $T(r)$  is required for the  $F$ -max procedure.

However, since the  $T(r)$  statistic is not automatically a pivotal quantity, i.e., its distribution can vary with  $r$ , the assumption of homogeneity of  $T(r)$  is not satisfied in general. In the presence of heterogeneity across different spatial points  $r$ , the power of the  $F$ -max test can be low in comparison to the global envelope tests of the previous section, as we will show in the simulation study.

#### 2.4. False discovery rate approach

Another possibility for multiple correction of pointwise  $p$ -values is to control the false discovery rate (FDR) (Benjamini and Hochberg, 1995) instead of controlling the family-wise error rate (FWER) as is done by all the previously described tests. Since the interest lies here in the rejection of hypothesis  $H_0$  only and not in particular pointwise tests which are responsible for the overall rejection, the two stage FDR procedure (Benjamini et al., 2006) collapses to the original FDR procedure. Also the resampling based FDR approach (Yekutieli and Benjamini, 1999) is not practically feasible in the case of high dimensional permutation methods due to computationally of such procedure, because the permutation method has to be applied on each resampled data. Due to these reasons, we only consider the original FDR method in this paper. The FDR method is applied on the set of  $p_r, r \in I$ , values in order to decide if there is any deviation from the null model among the pointwise  $p_r, r \in I$ , values.

### 3. Simulation experiment

To compare the power and robustness of the proposed methods and the existing multiple comparison methods under different scenarios, we generate synthetic imaging data mimicking real data from neuroimaging studies. We considered a categorical factor  $g$  (indicating group) taking the values 1 or 2 according the group to which the image belongs to, and a continuous factor  $z$  that was generated from the uniform distribution on  $(0, 1)$ . We simulated images  $Y(r)$  in the square window  $[-1, 1]^2$  on a grid of  $51 \times 51$  pixel resolution from the following GLM models:

$$\text{M0 : } Y(r) = \epsilon(r)$$

$$\text{M1 : } Y(r) = \exp(-10 \cdot \|r\|) \cdot g + \epsilon(r)$$

$$\text{M1' : } Y(r) = \exp(-200 \cdot \|r\|) \cdot g + \epsilon(r)$$

and

$$\text{M2 : } Y(r) = \exp(-10 \cdot \|r\|) \cdot (g + z) + \epsilon(r).$$

Here  $\|r\|$  denotes the Euclidean distance of the pixel to the origin and  $\epsilon(r)$  is a zero-mean correlated error. The model M0 has no factors and generates purely noisy images, the models M1 and M1' generate two groups of images depending on the categorical factor  $g$  and the model M2 generates images which depend on both the categorical and continuous factors. The models M1 and M1' correspond

to simple comparison of two groups of images, where the "bump" at the center of the image is two times higher for second group than for the first group. In the model M1' the area where the two groups differ is about hundred times smaller than in M1. The model M2 is similar to M1, but the groups are disturbed by the continuous factor  $z$ . The model M0 is a null model where the images in the two groups are from the same model (no factors) and it was used for estimating the significance levels of the different tests. The models M1, M1' and M2 were used for power estimation.

For both models M1 and M1', six different correlated error structures  $\epsilon(r)$  were considered:

- (a) Gaussian error  $\epsilon(r) = G_{0.15}(r)$ , where  $G_{0.15}(r)$  is a Gaussian random field  $G_\rho(r)$  with the exponential correlation structure with scale parameter  $\rho$  and standard deviation  $\sigma$  which will take several values,
- (b) bimodal error  $\epsilon(r) = \frac{1}{2}G_{0.15}(r)^{1/5}$ ,
- (c) inhomogeneous bimodal distribution  $\epsilon(r) = \frac{1}{4}G_{0.15}(r)^{1/5} \left( \frac{\|r\|}{2} + 1 \right)$ ,
- (d)  $\epsilon(r) = \mathbb{I}(\|r\| \leq 0.5)G_{0.15}(r) + \mathbb{I}(\|r\| > 0.5)\frac{1}{2}G_{0.15}(r)^{1/5}$ , i.e. inhomogeneous distribution over  $I$  with the normal and bimodal errors in the middle and periphery of the image, respectively,
- (e)  $\epsilon(r) = \mathbb{I}(\|r\| \leq 0.5)G_{0.05}(r) + \mathbb{I}(\|r\| > 0.5)G_{0.3}(r)$ , i.e. Gaussian distribution with inhomogeneity in the correlation structure (scale parameters 0.05 and 0.3 in the middle and periphery of the image),
- (f)  $\epsilon(r) = \mathbb{I}(\|r\| \leq 0.5)\frac{1}{2}G_{0.05}(r)^{1/5} + \mathbb{I}(\|r\| > 0.5)\frac{1}{2}G_{0.3}(r)^{1/5}$ , i.e. bimodal distribution with inhomogeneity in the correlation structure.

The homogeneous error distributions (a) and (b) represent cases where the assumptions of all methods are fulfilled. The bimodal error (b) represents a situation where the permutation inference is necessary because the assumptions needed for parametric methods are not met. The bimodal error corresponds to the sharp changes in the image, whereas Gaussian error corresponds to the smooth changes in the image. Further, the errors (c) and (d) are not homogeneous across the image and illustrate cases where the variability of the test statistic  $T(r)$  in the periphery of the image can mask the signal from the center of the image. On the other hand, the errors (e) and (f) are used to investigate the effect of inhomogeneity in the correlation structure on the results.

All the images in the simulation study had the resolution  $51 \times 51$  pixels only due to time constraints of simulations; the computation time of a permutation test in the simplest case took almost 2 minutes on a 2.0 GHz kernel employing 2000 permutations, which number of permutations was used throughout the whole simulation study. The estimated significance levels and powers were recorded for various cases for all studied multiple comparison methods, i.e. for

$F$ -max,  $p$ -min,  $p$ -min with randomized solution of ties ( $p$ -min-rand), FDR and finally the proposed extreme rank length method (ERL), continuous rank method (Cont) and area rank method (Area).

To capture the behavior of the methods for various levels of significance, seven different standard deviations  $\sigma_1 = 0.1$ ,  $\sigma_2 = 0.2$ ,  $\sigma_3 = 0.3$ ,  $\sigma_4 = 0.5$ ,  $\sigma_5 = 0.75$ ,  $\sigma_6 = 1$  and  $\sigma_7 = 1.25$  were used in all studied cases. Each model was simulated with ten images per group and each experiment was repeated 1000 times in order to obtain estimated significance levels and powers.

Tables 1, 2 and 3 show the results for models M0, M1 and M1' in a shorted way. The detailed results can be seen in the Appendix. The model M2 revealed consistent results with model M1, therefore we do not report them.

The estimated significance levels revealed the same structure for all errors (a)-(f) (Table 1). The  $p$ -min and FDR methods were enourmously conservative. Since the  $p$ -min-rand method just randomizes the ties and the serious conservativeness of the  $p$ -min procedure shows that there is a huge amount of ties, the  $p$ -min-rand method is mainly driven by randomization. The  $F$ -max and all our proposed methods achieved the preset significance level  $\alpha = 0.05$  in all cases. (The 95% confidence interval for 1000 simulations with success probability 0.05 is (0.037, 0.063).) The only exception was the error (c), where Cont was slightly conservative. Remind here that the assumption of homogeneity of  $F$ -max, Cont and Area is not fulfilled with errors (c)-(d) and that the assumption of homogeneity of autocorrelation of ERL and Area is not fulfilled with errors (e)-(f).

	M0a- $\sigma_1$	M0b- $\sigma_1$	M0c- $\sigma_1$	M0d- $\sigma_1$	M0e- $\sigma_1$	M0f- $\sigma_1$
F-max	0.054	0.0555	0.040	0.046	0.058	0.043
$p$ -min	0.000	0.000	0.000	0.000	0.000	0.000
FDR	0.000	0.000	0.000	0.000	0.002	0.000
$p$ -min-rand	0.044	0.047	0.059	0.054	0.047	0.042
ERL	0.060	0.052	0.045	0.043	0.057	0.045
Cont	0.058	0.056	0.031	0.043	0.049	0.053
Area	0.058	0.047	0.040	0.040	0.061	0.045

Table 1: Estimated significance levels of all studied methods for model M0 with error (a)-(f) with standard deviation  $\sigma_1 = 0.1$ .

The conservative  $p$ -min method had no power (Tables 2 and 3). The  $p$ -min-rand procedure was again driven by huge amount of pure randomness leading to low power. The ERL and Area methods had uniformly higher power than  $F$ -max and FDR for all errors in case of the model M1. This is caused by the fact that ERL and Area summarize the extremeness of the test statistic from all spatial points. This advantage led to higher power even in the cases (e)-(f) with inhomogeneous autocorrelation.

The situation is more complicated for model M1', where the area of extremeness is rather small: the ERL and Area can not benefit from their feature of collecting information from all spatial points. For normal homogeneous case

	M1a- $\sigma_5$	M1b- $\sigma_7$	M1c- $\sigma_7$	M1d- $\sigma_4$	M1e- $\sigma_5$	M1f- $\sigma_6$
F-max	0.395	0.243	0.224	0.364	0.632	0.421
$p$ -min	0.000	0.000	0.000	0.000	0.000	0.000
FDR	0.062	0.314	0.320	0.570	0.001	0.523
$p$ -min-rand	0.072	0.099	0.093	0.076	0.090	0.084
ERL	0.606	0.915	0.922	0.953	0.776	0.984
Cont	0.378	0.238	0.203	0.367	0.522	0.358
Area	0.544	0.857	0.863	0.923	0.749	0.979

Table 2: Estimated powers of all studied methods for model M1 with error (a)-(f). The chosen standart deviation  $\sigma$  for each case is the one with maximal contrast between methods.

	M1'a- $\sigma_3$	M1'b- $\sigma_1$	M1'c- $\sigma_2$	M1'd- $\sigma_4$	M1'e- $\sigma_3$	M1'f- $\sigma_1$
F-max	0.917	0.350	0.177	0.086	0.963	0.412
$p$ -min	0.000	0.000	0.000	0.000	0.000	0.000
FDR	0.000	0.000	0.000	0.000	0.002	0.000
$p$ -min-rand	0.081	0.099	0.077	0.067	0.113	0.088
ERL	0.732	0.961	0.682	0.210	0.720	0.894
Cont	0.799	0.346	0.184	0.092	0.899	0.408
Area	0.825	0.877	0.580	0.214	0.924	0.924

Table 3: Estimated powers of all studied methods for model M1' with error (a)-(f). The chosen standart deviation  $\sigma$  for each case is the one with maximal contrast between methods.

(a) and normal homogeneous case with inhomogeneous autocorrelation (e), the  $F$ -max is the most powerful, but when deviating from this ideal ' $F$ -max' state, the ERL and Area were the most powerful methods (Table 3). The Cont and  $F$ -max methods were rather equivalent in our study with 2601 spatial points and 2000 permutations. The FDR method had very poor power for model M1'.

#### 4. A simulated example

To illustrate the proposed method, we generated an artificial example of two groups of ten images, where each image was generated according to the model M2 with the error structure (d) of the simulation experiment using the standard deviation  $\sigma_2 = 0.2$ . We then performed the permutation inference for the GLM with the two factors keeping each of them as the regressor of interest on its turn and calculated the  $F$ -statistic for the null hypothesis  $\beta(r) = 0$  at each spatial point  $r \in [-1, 1]^2$  for the data and for each permutation. Figure 2 shows the test result for the discrete (upper row) and continuous factors (lower row) using the global area rank envelope. The significant difference between the groups is realized in the middle of the image as supposed. Similarly, the continuous factor has significant effect in the middle of the image.

Note how the error distribution is reflected in the upper area rank envelope (Figure 2, middle): The upper envelope obtains higher values in the periphery of the image, thus adjusting for the difference in the distribution across the

image. On the other hand, the  $F$ -max test is based on a constant critical value, which partly explains why it had lower power than the rank based tests in the case of inhomogeneous error structure.

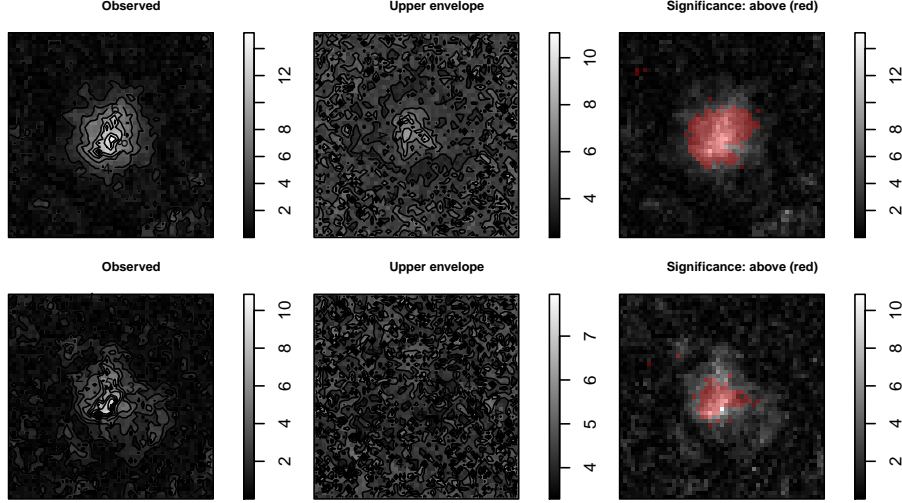


Figure 2: Observed  $F$ -statistic (left), upper 95% global area rank envelope (middle) and the significant effects (right) for the simulated example of two groups with ten images and a confounding continuous factor. For visualisation, the values in the images have been square-root transformed. Upper row: test results for the discrete *group* factor; lower row: the test results for the continuous factor.

## 5. Conclusions and discussion

We presented three new multiple comparison methods for the permutation inference for the GLM. We showed by a designed experiment that the proposed methods have the desired significance level unlike the  $p$ -min method that was highly conservative. The proposed and  $F$ -max methods had also uniformly higher power than FDR, which is due to the fact that our methods and  $F$ -max use information about the correlation structure of the test statistic across the image obtained from permutations whereas FDR is a general multiple comparison method which due to its generality can not use this information.

The choice of the method from  $F$ -max, extreme rank length (ERL), continuous (Cont) and area rank (Area) measures should depend on the assumptions that can be made and the expected type of extremeness of the test statistic. When we assume

- homogeneity of the distribution of  $T(r)$  and homogeneity of the correlation structure of  $T(r)$ , then all methods can be applied. The ERL or Area methods should be preferred when the test statistic is expected to be extreme over a large area of the image  $I$ ,  $F$ -max, Cont or Area when

extremeness is expected only on a small area. The same recommendations hold, if the assumption of homogeneity of  $T(r)$  is replaced by the assumption of the normality of the error  $\epsilon(r)$ .

- homogeneity of the correlation structure of  $T(r)$  across the image (but not homogeneity of the distribution), then only ERL can be applied without conflicting its assumptions. However, in our designed experiment, Area showed good robustness with respect to violating the assumption of homogeneity of the distribution of  $T(r)$ , whereas  $F$ -max and Cont did not.
- homogeneity of the distribution of  $T(r)$  (but not homogeneity of the correlation structure), then  $F$ -max and Cont can be applied without conflicting their assumptions. Again Area showed good robustness with respect to violating the assumption of homogeneity of the correlation structure of  $T(r)$ , whereas ERL did not.
- nothing, then none of the methods can be applied without conflicting their assumptions, but Area showed good robustness with respect to violating both assumptions.

Thus, our experience suggests that the Area method can be used in a general situation without worry of losing much power. Its dual nature of being based both on extremeness of the test statistic as well as on summarizing this extremeness from all spatial points makes it sensitive to different departures from the null model and robust to different kinds of inhomogeneity.

From all the above mentioned reasons we have found the ERL and Area methods very useful for the neuroimage practice.

## Acknowledgements

T. Mrkvička has been financially supported by the Grant Agency of Czech Republic (Project No. 19-04412S) and M. Myllymäki by the Academy of Finland (project numbers 295100, 306875).

## References

## References

- Anderson, M., Ter Braak, C., 2003. Permutation tests for multi-factorial analysis of variance. *Journal of Statistical Computation and Simulation* 73, 85 – 113.
- Benjamini, Y., Hochberg, Y., 1995. Controlling the false discovery rate: A practical and powerful approach to multiple testing. *Journal of the Royal Statistical Society. Series B (Methodological)* 57, 289–300. URL: <http://www.jstor.org/stable/2346101>.

- Benjamini, Y., Krieger, A., M., Yekutieli, D., 2006. Adaptive linear step-up procedures that controls the false discovery rate. *Biometrika* 93, 491 – 507.
- Christensen, R., 2002. *Plane Answers to Complex Questions*. Springer.
- Fisher, R.A., 1935. *The design of experiments*. Oliver & Boyd.
- Freedman, D., Lane, D., 1983. A nonstochastic interpretation of reported significance levels. *Journal of Business and Economic Statistics* 1, 292–298.
- Hahn, U., 2015. A note on simultaneous Monte Carlo tests. Technical Report. Centre for Stochastic Geometry and advanced Bioimaging, Aarhus University.
- Hayasaka, S., Phan, K., Liberzon, I., Worsley, K.J., Nichols, T.E., 2004. Nonstationary cluster-size inference with random field and permutation methods. *NeuroImage* 22, 676–687. URL: <http://www.sciencedirect.com/science/article/pii/S1053811904000862>, doi:<https://doi.org/10.1016/j.neuroimage.2004.01.041>.
- Mrkvička, T., Myllymäki, M., Hahn, U., 2016. Multiple monte carlo testing, with applications in spatial point processes. *Statistics and Computing*, Doi: 10.1007/s11222-016-9683-9 URL: <http://dx.doi.org/10.1007/s11222-016-9683-9>, doi:10.1007/s11222-016-9683-9, arXiv:arXiv:1307.0239 [stat.ME].
- Mrkvička, T., Myllymäki, M., Jílek, M., Hahn, U., 2018. A one-way anova test for functional data with graphical interpretation URL: <https://arxiv.org/abs/1612.03608>, arXiv:arXiv:1612.03608 [stat.ME].
- Myllymäki, M., Mrkvička, T., Grabarnik, P., Seijo, H., Hahn, U., 2017. Global envelope tests for spatial processes. *J. R. Statist. Soc. B* 79, 381 – 404. doi:10.1111/rssb.12172, arXiv:arXiv:1307.0239 [stat.ME].
- Narisetty, N.N., Nair, V.N., 2016. Extremal depth for functional data and applications. *Journal of American Statistical Association* 111, 1705–1714.
- Pantazis, D., Nichols, T.E., Baillet, S., Leahya, R.M., 2005. A comparison of random field theory and permutation methods for the statistical analysis of meg data. *Neuroimage* 25, 383–394.
- Salimi-Khorshidi, G., Smith, S.M., Nichols, T.E., 2011. Adjusting the effect of nonstationarity in cluster-based and tfce inference. *NeuroImage* 54, 2006–2019. URL: <http://www.sciencedirect.com/science/article/pii/S1053811910012917>, doi:<https://doi.org/10.1016/j.neuroimage.2010.09.088>.
- Winkler, A., Ridgway, G., Webster, M., Smith, S., Nichols, T., 2014. Permutation inference for the general linear model. *Neuroimage* 92, 381–97.
- Yekutieli, D., Benjamini, Y., 1999. Resampling-based false discovery rate controlling multiple test procedures for correlated test statistics. *Journal of Statistical Planning and Inference* 82, 171 – 196.

## Appendix

The following tables contain all results of the simulation study for M1 and M1'.

	$\sigma_1$	$\sigma_2$	$\sigma_3$	$\sigma_4$	$\sigma_5$	$\sigma_6$	$\sigma_7$
F-max	0.054	0.048	0.043	0.051	0.044	0.045	0.047
$p$ -min	0.000	0.000	0.000	0.000	0.000	0.000	0.000
FDR	0.000	0.000	0.000	0.000	0.000	0.000	0.000
$p$ -min-rand	0.044	0.051	0.051	0.050	0.051	0.045	0.040
ERL	0.060	0.036	0.042	0.048	0.052	0.046	0.040
Cont	0.058	0.060	0.047	0.042	0.052	0.055	0.047
Area	0.058	0.040	0.041	0.053	0.047	0.050	0.040

Table 4: Estimated significance levels of all studied methods and 7 standart deviations for model M0 with error (a).

	$\sigma_1$	$\sigma_2$	$\sigma_3$	$\sigma_4$	$\sigma_5$	$\sigma_6$	$\sigma_7$
F-max	1.000	1.000	1.000	0.863	0.395	0.184	0.106
$p$ -min	0.000	0.000	0.000	0.000	0.000	0.000	0.000
FDR	1.000	1.000	1.000	0.540	0.062	0.009	0.002
$p$ -min-rand	0.094	0.080	0.079	0.072	0.063	0.077	0.057
ERL	0.979	0.975	0.980	0.943	0.606	0.292	0.188
Cont	0.979	0.975	0.980	0.824	0.378	0.170	0.105
Area	0.979	0.975	0.980	0.929	0.544	0.257	0.150

Table 5: Estimated powers of all studied methods and 7 standart deviations for model M1 with error (a).

	$\sigma_1$	$\sigma_2$	$\sigma_3$	$\sigma_4$	$\sigma_5$	$\sigma_6$	$\sigma_7$
F-max	0.931	0.722	0.557	0.427	0.311	0.256	0.243
$p$ -min	0.000	0.000	0.000	0.000	0.000	0.000	0.000
FDR	1.000	1.000	0.998	0.960	0.718	0.441	0.314
$p$ -min-rand	0.073	0.075	0.078	0.078	0.066	0.083	0.099
ERL	0.976	0.970	0.972	0.980	0.981	0.956	0.915
Cont	0.894	0.726	0.540	0.404	0.285	0.233	0.238
Area	0.976	0.970	0.972	0.978	0.952	0.906	0.857

Table 6: Estimated powers of all studied methods and 7 standart deviations for model M1 with error (b).

	$\sigma_1$	$\sigma_2$	$\sigma_3$	$\sigma_4$	$\sigma_5$	$\sigma_6$	$\sigma_7$
F-max	0.920	0.731	0.573	0.405	0.324	0.275	0.224
$p$ -min	0.000	0.000	0.000	0.000	0.000	0.000	0.000
FDR	1.000	0.999	1.000	0.955	0.686	0.448	0.320
$p$ -min-rand	0.083	0.084	0.088	0.087	0.079	0.090	0.093
ERL	0.979	0.976	0.982	0.983	0.971	0.953	0.922
Cont	0.921	0.707	0.535	0.368	0.296	0.245	0.203
Area	0.979	0.976	0.982	0.978	0.943	0.893	0.863

Table 7: Estimated powers of all studied methods and 7 standart deviations for model M1 with error (c).

	$\sigma_1$	$\sigma_2$	$\sigma_3$	$\sigma_4$	$\sigma_5$	$\sigma_6$	$\sigma_7$
F-max	1.000	1.000	0.986	0.364	0.075	0.059	0.050
$p$ -min	0.000	0.000	0.000	0.000	0.000	0.000	0.000
FDR	1.000	1.000	1.000	0.570	0.051	0.004	0.000
$p$ -min-rand	0.091	0.099	0.081	0.076	0.087	0.065	0.052
REF	0.984	0.979	0.978	0.953	0.593	0.303	0.161
Cont	0.984	0.979	0.950	0.367	0.089	0.062	0.061
Area	0.984	0.979	0.978	0.923	0.472	0.232	0.136

Table 8: Estimated powers of all studied methods and 7 standart deviations for model M1 with error (d).

	$\sigma_1$	$\sigma_2$	$\sigma_3$	$\sigma_4$	$\sigma_5$	$\sigma_6$	$\sigma_7$
F-max	1.000	1.000	1.000	0.998	0.632	0.296	0.143
$p$ -min	0.000	0.000	0.000	0.000	0.000	0.000	0.000
FDR	1.000	1.000	1.000	0.701	0.001	0.001	0.000
$p$ -min-rand	0.102	0.096	0.105	0.084	0.090	0.095	0.075
ERL	0.981	0.980	0.985	0.985	0.776	0.325	0.126
Cont	0.981	0.980	0.985	0.971	0.522	0.249	0.129
Area	0.981	0.980	0.985	0.984	0.749	0.340	0.141

Table 9: Estimated powers of all studied methods and 7 standart deviations for model M1 with error (e).

	$\sigma_1$	$\sigma_2$	$\sigma_3$	$\sigma_4$	$\sigma_5$	$\sigma_6$	$\sigma_7$
F-max	0.999	0.950	0.841	0.658	0.522	0.421	0.352
$p$ -min	0.000	0.000	0.000	0.000	0.000	0.000	0.000
FDR	1.000	1.000	0.999	0.988	0.852	0.523	0.254
$p$ -min-rand	0.094	0.084	0.089	0.088	0.093	0.084	0.081
ERL	0.986	0.980	0.977	0.979	0.981	0.984	0.978
Cont	0.985	0.917	0.790	0.604	0.448	0.358	0.300
Area	0.986	0.980	0.977	0.979	0.981	0.979	0.970

Table 10: Estimated powers of all studied methods and 7 standart deviations for model M1 with error (f).

	$\sigma_1$	$\sigma_2$	$\sigma_3$	$\sigma_4$	$\sigma_5$	$\sigma_6$	$\sigma_7$
F-max	1.000	1.000	0.917	0.277	0.089	0.068	0.045
$p$ -min	0.000	0.000	0.000	0.000	0.000	0.000	0.000
FDR	0.017	0.001	0.000	0.000	0.000	0.000	0.000
$p$ -min-rand	0.070	0.089	0.085	0.071	0.053	0.054	0.052
ERL	0.975	0.976	0.732	0.201	0.071	0.064	0.052
Cont	0.975	0.975	0.799	0.230	0.077	0.058	0.048
Area	0.975	0.980	0.825	0.254	0.085	0.068	0.049

Table 11: Estimated powers of all studied methods and 7 standart deviations for model M1' with error (a).

	$\sigma_1$	$\sigma_2$	$\sigma_3$	$\sigma_4$	$\sigma_5$	$\sigma_6$	$\sigma_7$
F-max	0.350	0.171	0.101	0.081	0.079	0.061	0.050
$p$ -min	0.000	0.000	0.000	0.000	0.000	0.000	0.000
FDR	0.000	0.000	0.000	0.000	0.000	0.000	0.000
$p$ -min-rand	0.081	0.081	0.071	0.082	0.078	0.080	0.064
ERL	0.961	0.686	0.376	0.255	0.237	0.185	0.171
Cont	0.346	0.171	0.101	0.074	0.067	0.060	0.047
Area	0.877	0.576	0.384	0.280	0.219	0.154	0.156

Table 12: Estimated powers of all studied methods and 7 standart deviations for model M1' with error (b).

	$\sigma_1$	$\sigma_2$	$\sigma_3$	$\sigma_4$	$\sigma_5$	$\sigma_6$	$\sigma_7$
F-max	0.349	0.177	0.118	0.081	0.090	0.078	0.053
$p$ -min	0.000	0.000	0.000	0.000	0.000	0.000	0.000
FDR	0.000	0.000	0.000	0.000	0.000	0.000	0.000
$p$ -min-rand	0.080	0.077	0.079	0.090	0.081	0.066	0.057
ERL	0.958	0.682	0.394	0.255	0.214	0.176	0.162
Cont	0.338	0.184	0.130	0.093	0.078	0.071	0.060
Area	0.869	0.580	0.410	0.282	0.224	0.159	0.133

Table 13: Estimated powers of all studied methods and 7 standart deviations for model M1' with error (c).

	$\sigma_1$	$\sigma_2$	$\sigma_3$	$\sigma_4$	$\sigma_5$	$\sigma_6$	$\sigma_7$
F-max	1.000	0.985	0.548	0.086	0.048	0.043	0.048
$p$ -min	0.000	0.000	0.000	0.000	0.000	0.000	0.000
FDR	0.012	0.002	0.000	0.000	0.000	0.000	0.000
$p$ -min-rand	0.075	0.073	0.075	0.067	0.062	0.040	0.038
ERL	0.979	0.970	0.753	0.210	0.082	0.061	0.052
Cont	0.979	0.905	0.461	0.092	0.045	0.057	0.047
Area	0.979	0.968	0.783	0.214	0.077	0.069	0.053

Table 14: Estimated powers of all studied methods and 7 standart deviations for model M1' with error (d).

	$\sigma_1$	$\sigma_2$	$\sigma_3$	$\sigma_4$	$\sigma_5$	$\sigma_6$	$\sigma_7$
F-max	1.000	1.000	0.963	0.358	0.089	0.058	0.057
$p$ -min	0.000	0.000	0.000	0.000	0.000	0.000	0.000
FDR	0.017	0.003	0.002	0.000	0.002	0.001	0.001
$p$ -min-rand	0.091	0.079	0.113	0.077	0.062	0.045	0.053
ERL	0.975	0.978	0.720	0.110	0.059	0.051	0.045
Cont	0.975	0.979	0.899	0.275	0.083	0.062	0.047
Area	0.975	0.979	0.924	0.258	0.077	0.056	0.048

Table 15: Estimated powers of all studied methods and 7 standart deviations for model M1' with error (e).

	$\sigma_1$	$\sigma_2$	$\sigma_3$	$\sigma_4$	$\sigma_5$	$\sigma_6$	$\sigma_7$
F-max	0.412	0.228	0.146	0.101	0.084	0.073	0.067
$p$ -min	0.000	0.000	0.000	0.000	0.000	0.000	0.000
FDR	0.000	0.000	0.001	0.000	0.000	0.001	0.000
$p$ -min-rand	0.088	0.077	0.092	0.085	0.090	0.073	0.070
ERL	0.894	0.589	0.311	0.193	0.186	0.132	0.120
Cont	0.408	0.189	0.124	0.094	0.081	0.063	0.073
Area	0.924	0.612	0.424	0.292	0.208	0.154	0.134

Table 16: Estimated powers of all studied methods and 7 standart deviations for model M1' with error (f).